



Available online at [www.sciencedirect.com](http://www.sciencedirect.com)

SCIENCE @ DIRECT®

Journal of Hydrology 277 (2003) 214–229

Journal  
of  
Hydrology

[www.elsevier.com/locate/jhydrol](http://www.elsevier.com/locate/jhydrol)

# Calibration and sensitivity analysis of a river water quality model under unsteady flow conditions

Andrew M. Sincok<sup>a,\*</sup>, Howard S. Wheater<sup>a</sup>, Paul G. Whitehead<sup>b</sup>

<sup>a</sup>*Department of Civil and Environmental Engineering, Imperial College of Science, Technology and Medicine, Imperial College Road, London SW7 2BU, UK*

<sup>b</sup>*Department of Geography, University of Reading, Reading RG6 6AB, UK*

Received 13 June 2001; accepted 13 March 2003

## Abstract

Water quality models generally require a relatively large number of parameters to define their functional relationships, and since prior information on parameter values is limited, these are commonly defined by fitting the model to observed data. In this paper, the identifiability of water quality parameters and the associated uncertainty in model simulations are investigated. A modification to the water quality model ‘Quality Simulation Along River Systems’ is presented in which an improved flow component is used within the existing water quality model framework. The performance of the model is evaluated in an application to the Bedford Ouse river, UK, using a Monte-Carlo analysis toolbox. The essential framework of the model proved to be sound, and calibration and validation performance was generally good. However some supposedly important water quality parameters associated with algal activity were found to be completely insensitive, and hence non-identifiable, within the model structure, while others (nitrification and sedimentation) had optimum values at or close to zero, indicating that those processes were not detectable from the data set examined.

© 2003 Elsevier Science B.V. All rights reserved.

*Keywords:* Bedford Ouse; Nitrate; DO; BOD; Quality Simulation Along River Systems; Water quality modelling

## 1. Introduction

The ability to predict accurately dynamic water quality behaviour in rivers is essential to address problems characterised by unsteady river flow conditions such as the control of combined sewer overflows and the prediction of point source pollutant spills. Here we investigate the dynamic performance

of an extension of a well-established water quality model, QUASAR (Whitehead et al., 1997), which is typical of many water quality models in using continuously stirred tank reactors (CSTRs) as a basis for both flow and water quality modelling. In this application, a modified flow component, which allows for the difference between solute and flood wave velocity, is used to improve the model capability to simulate unsteady flows (Sincok and Lees, 2002).

The combination of uncertainty in parameter values within a water quality model structure, error associated with the model structure and error in

\* Corresponding author. Tel.: +44-7949039977; fax: +44-2075946124.

E-mail address: [a.sincok@ic.ac.uk](mailto:a.sincok@ic.ac.uk) (A.M. Sincok).

the observed data leads to uncertainty in the model predictions, which should ideally be represented as an integral part of the model output. There is therefore a need for appropriate methods to represent output uncertainty, and for techniques to investigate model performance in terms of parameter sensitivity and identifiability (see e.g. [Wheater et al., 1993](#); [Wheater and Beck, 1995](#); [Wagener et al., 2001](#)). If sensitive parameters are not identifiable there will be a high level of uncertainty associated with parameter values and a consequent high level of output uncertainty. Parameter identifiability generally decreases with increasing parameter numbers and is therefore a particular issue for water quality models, which tend to be complex, due to the need to represent multiple processes and multiple outputs. In addition, if there is a high degree of uncertainty associated with the value of a parameter, it will be difficult to assign physical significance to the parameter, interpret field data using the model or transfer parameter values between applications.

It should be noted that for models of only modest complexity, different combinations of model parameter values (and even different model structures) are capable of producing outputs with similar performance statistics, an effect known as ‘equifinality’ ([Beven and Binley, 1992](#)). Hence it has been proposed ([Hornberger and Spear, 1981](#); [Spear and Hornberger, 1980](#); [Beven, 2000](#)) that if we accept that there is no single correct or optimal model, then one may adopt an alternative approach in which the likelihood that a particular model/parameter set is consistent with the available data is quantified. The essence of such an approach is captured in the Generalised Likelihood Uncertainty Estimation (GLUE) methodology ([Beven and Binley, 1992](#)), which provides a basis for estimating confidence limits for model outputs.

Part of the lack of uniqueness lies in the use of a single criterion for model performance; recently attention has been focussed on the use of multiple performance criteria, to extract more information from a single output time-series, or from multiple outputs ([Gupta et al., 1998](#); [Wagener et al., 2001](#)). This additional information can be used to improve parameter identifiability, and to investigate trade-offs in performance between different criteria, and hence model inconsistencies and structural weaknesses.

It follows that a procedure for model development and evaluation is required which investigates parameter sensitivity, identifiability and uncertainty, seeking an optimal trade-off between performance and identifiability for a given application. Here we use the Monte-Carlo Analysis Toolbox (MCAT), developed at Imperial College ([Lees and Wagener, 2000](#)), to investigate model performance.

## 2. The QUASAR water quality model

QUASAR is a simple conceptual Cells In Series model based on the conservation of mass for water and solute within a completely mixed cell. It is a lumped representation of a completely mixed river system, with each cell in the cascade consisting of a single CSTR. Within QUASAR the water quality component is based on such a cascade in which changes in nitrate, ammonium, temperature, BOD and DO are modelled. DO is added to the system by modelling algae, aquatic plants and phytoplankton which utilise water, carbon dioxide and sunlight to photosynthesize, with the resultant oxygen being released into the water column. Respiration, which depletes the DO store in the water, occurs through the day. These two processes result in the highest DO concentration at mid-afternoon and the lowest concentration during the early hours of the morning. Loss of oxygen is via algae respiration and by benthic oxygen demand (river bed or mud respiration). Oxygen is added to the system by the reaeration of the river at the surface. If there is ammonium in the water column this will be converted to nitrate. During this reaction oxygen is also consumed. Thus, there is a term for oxygen depletion as a result of nitrification. The biochemical oxygen demand is caused by the decay of organic material in the stream. As the material decays it consumes oxygen, thus the model contains a term for oxygen depletion due to BOD decay.

QUASAR models both carbonaceous BOD and nitrogenous BOD separately with the nitrogenous BOD having been described above. The change in carbonaceous biochemical oxygen is due to decay, sedimentation and addition due to dead algae. As algae die they contribute to the BOD; the rate of contribution is proportional to the product of the concentration of algae and the rate of BOD addition by dead algae. The flow variable average residence time is used in

the calculation of all the determinands within QUA-SAR, namely temperature, ammonium, nitrate, BOD and DO (Whitehead et al., 1997):

### 2.1. Temperature

$$\frac{d(T_1)}{dt} = \frac{U_1 + P_1 - T_1}{T_p} \quad (1)$$

where

- $U_1$  input temperature (°C)
- $P_1$  additional input temperature from tributaries, spillages, etc. (°C)
- $T_1$  reach and output temperature (°C)
- $T_p$  residence time (s)

### 2.2. Ion ammonium concentration

$$\frac{d(X_2)}{dt} = \frac{U_2 + P_2 - X_2}{T_p} - [K_1^0 \times 10^{(0.0293T_1)} X_2] \quad (2)$$

where

- $U_2$ , input ammonium concentration (mg l<sup>-1</sup>)
- $P_2$  additional input ammonium concentration from tributaries, etc. (mg l<sup>-1</sup>)
- $X_2$  reach and output ammonium concentration (mg l<sup>-1</sup>)
- $K_1^0$  nitrification rate coefficient at 20 °C (day<sup>-1</sup>)

### 2.3. Nitrate concentration

$$\frac{d(X_3)}{dt} = \frac{U_3 + P_3 - X_3}{T_p} + [K_1^0 \times 10^{(0.0293T_1)} X_2] - [K_2^0 \times 1.0698 \times 10^{(0.0293T_1)} X_3] \quad (3)$$

where

- $U_3$  input nitrate concentration (mg l<sup>-1</sup>)
- $P_3$  additional input nitrate concentration from tributaries, spillages, etc. (mg l<sup>-1</sup>)
- $X_3$  reach and output nitrate concentration (mg l<sup>-1</sup>)
- $K_2^0$  denitrification rate coefficient at 20 °C (day<sup>-1</sup>)

### 2.4. Biochemical oxygen demand concentration

$$\frac{d(X_4)}{dt} = \frac{U_4 + P_4 - X_4}{T_p} - [K_5^0 \times 1.047^{(T_1-20)} X_4] - [K_{10} X_4] + [K_{11} \cdot \text{Cla}] \quad (4)$$

where

- $U_4$  input BOD concentration (mg l<sup>-1</sup>)
- $P_4$  additional input BOD concentration from tributaries, spillages, etc. (mg l<sup>-1</sup>)
- $X_4$  reach and output BOD concentration (mg l<sup>-1</sup>)
- $K_5^0$  rate coefficient for the loss of BOD at 20 °C (day<sup>-1</sup>)
- $K_{10}$  sedimentation rate coefficient (day<sup>-1</sup>)
- $K_{11}$  BOD contribution by algae rate coefficient (day<sup>-1</sup>)
- Cla reach Chlorophyll-a concentration (mg l<sup>-1</sup>)

### 2.5. Dissolved oxygen concentration

$$\frac{d(X_5)}{dt} = \frac{U_5 - X_5 + \text{Weir}}{T_p} + P - [(K_8 + K_9 \cdot \text{Cla}) \times 1.08^{(T_1-20)}] - [K_3^0 \times 1.08^{(T_1-20)} X_5] + [((5.32v^{0.67} 1.024^{(T_1-20)}) / (d^{1.85})) \times (\text{SC} - X_5)] - [4.57 K_1^0 \times 10^{(0.0293T_1)} X_2] - [K_5^0 \times 1.047^{(T_1-20)} X_4] \quad (5)$$

where

- $U_5$  input DO concentration (mg l<sup>-1</sup>)
- $X_5$  reach and output DO concentration (mg l<sup>-1</sup>)
- Weir increase in oxygen concentration due to aeration over a weir
- $P$  reach photosynthetic oxygen production (mg l<sup>-1</sup>)
- $K_8$  algae respiration coefficient (day<sup>-1</sup>)
- $K_9$  algae respiration coefficient as a direct proportion of Chlorophyll-a (day<sup>-1</sup>)
- $K_3^0$  rate of oxygen uptake by sediment at 20 °C (day<sup>-1</sup>)
- $v$  stream velocity (m/s)

$d$  river depth (m)  
 SC saturation concentration for DO ( $\text{mg l}^{-1}$ )

### 3. Flow model component

The original QUASAR model (Whitehead et al., 1997) is only applicable to slowly time-varying flow (quasi steady-state) conditions, since the flow and solute travel times are assumed equal. However, under unsteady conditions, the travel time of a flow wave can be approximated by the kinematic wave velocity (celerity), which is greater than the water velocity. An improved flow model can thus be formulated based on celerity and not velocity. In the case of the Bedford Ouse (with only daily data being available at exact 24 h intervals) a quasi steady-state model may suffice, however a truly generic unsteady flow model is utilised here in order to progress the state of the art and allow future applications to data sets of higher quality.

The ratio  $m$  of the average kinematic wave speed, or celerity  $c$ , to the average velocity of flow,  $u$ , is given by

$$m = \frac{c}{u} = \frac{\left(\frac{dQ}{dA}\right)}{\left(\frac{Q}{A}\right)} \quad (6)$$

where  $Q$  is discharge and  $A$  is the cross sectional area of flow. Note that for a wide rectangular channel  $m$  may be approximated to 5/3 (Chapra, 1997).

A number of recent research developments have been made in the area of hydrological flow routing (Bentura and Michel, 1997; Permual, 1994; Camacho and Lees, 1999). The main advance that these developments have introduced is the inclusion of a non-linear method of flood routing coupled with a lag term. The increased flexibility and accuracy that such approaches represent has led to this concept being adopted here, building on Bentura and Michel's lag and quadratic route model. The flow model can be conceptualised as a series of  $n$  non-linear stores followed by a time delay parameter,  $\tau_{fl}$ , the effect of which is simply to lag the routed hydrograph without attenuation (Camacho and Lees, 1999). Note that  $\tau_{fl}$  varies with respect to discharge via a non-linear

relationship, where  $\tau_{fl} = cQ^d$ . Each non-linear store in the cascade in turn is characterised by a storage coefficient  $K$  and an exponent  $\alpha$  (where  $0 < \alpha \leq 1$ , note that  $\alpha = 1$  equates to the linear case and  $\alpha = 0.5$  equates to the quadratic case). Hence to allow for non-linearity in each storage reservoir the storage–discharge relationship is expressed as

$$S = KQ^\alpha \quad (7)$$

For  $S$  (storage) in  $\text{m}^3$  and  $Q$  in  $\text{m}^3/\text{s}$  the factor  $K$  has the dimension  $\text{m}^{3-3\alpha}\text{s}^\alpha$ . Note that an attractive feature of the linear reservoir (the unique case where  $\alpha = 1$ ) is that the storage coefficient,  $K$ , which is also equal to the ratio of  $S/Q$ , can be directly interpreted as representative of average travel time of the flow in units of seconds. The storage coefficient,  $k_{nl}$ , for a non-linear store may also be expressed as the ratio of  $S/Q$

$$k_{nl} = \frac{S}{Q} = KQ^{\alpha-1} \quad (8)$$

hence the overall travel time,  $T$ , of the flow wave is given by

$$T = nk_{nl} + \tau_{fl} \quad (9)$$

The celerity,  $c$ , of the flow wave for the reach length under consideration,  $L$ , is given by

$$c = \frac{L}{nk_{nl} + \tau_{fl}} \quad (10)$$

where  $\tau_{fl}$  varies with respect to discharge,  $\tau_{fl} = cQ^d$ . Hence the travel time of the non-conservative pollutant,  $T_p$ , is given by

$$T_p = m(nk_{nl} + \tau_{fl}) \quad (11)$$

It is this residence time that is utilised in Eqs. (1)–(5) in the evaluation of these water quality determinands.

### 4. Numerical simulation and calibration methods

Calibration is carried out here in a two-step procedure in which the flow parameters are first optimised with respect to flow, prior to calibration of the water quality relationships. The flow and water quality components of the model are simulated using standard numerical integration techniques, in this case the adaptive step size fourth order Runge–Kutta

algorithm provided in the MATLAB numerical software package (Mathworks, 1996). The flow component is optimised on a reach by reach basis between stream flow gauging stations in the downstream direction in order to obtain the optimum flow model parameters  $K$ ,  $\alpha$ ,  $c$ ,  $d$  (where  $k_{nl} = KQ^{\alpha-1}$  and  $\tau_{nl} = cQ^d$ ) for an optimum number of cells,  $n$ , determined by direct calibration (i.e. trials of number of cells ranged from 1 upwards until no performance advantage was gained by increasing the number of cells further), with the reach length being that utilised in Eqs. (1)–(5).

Both the flow and water quality components of the model were calibrated using the MCAT developed at Imperial College (Lees and Wagener, 2000). Some of the functionality of the MCAT is describe here in the context of assessing the sensitivity and identifiability of this model. The MCAT uses a series of graphical techniques to display Monte-Carlo results and support analysis of model performance.

MCAT uses Regional Sensitivity Analysis (RSA) (Hornberger and Spear, 1981; Spear and Hornberger, 1980) to assess the sensitivity of model parameters, where sensitivity is defined as the effect of changes in the parameters on the overall model performance (as indicated by an objective function (for example the Nash–Sutcliffe criteria—Nash and Sutcliffe, 1970)). One of the approaches adopted in the MCAT uses the extension to RSA introduced by Freer et al. (1996). Essentially parameter sets are drawn at random from prior distributions of feasible values (which may simply be taken from a uniform distribution) and used for Monte-Carlo simulations. Simulations are ranked according to the selected objective function, and split between a behavioural set, which are feasibly consistent with the data support, and a non-behavioural set, which is discarded as being a totally unrealistic representation of the system (as judged by an objective function). A model fit is considered ‘behavioural’ if the corresponding objective function is within a selected threshold, for example a threshold of Nash–Sutcliffe  $R^2 = 0$  (Nash and Sutcliffe, 1970), all other results are considered ‘non-behavioural’—i.e. the response deviates so far from the observations that the model cannot be considered to be a possible characterisation of the system. The objective functions are then transformed into likelihood values (i.e. the chance of

occurrence) split into ten quantile groups and the cumulative frequency distribution is calculated and plotted (Wagener et al., 2001). If the model performance is sensitive to a particular parameter there will be a large difference between the cumulative frequency distributions of the quantile groups. If the model performance is not sensitive to a particular parameter, given an a priori uniform distribution each group will plot on a straight line (Wagener et al., 2001).

Sensitivity is only one of the essential requirements of an identifiable parameter. A parameter is termed identifiable if it is possible to determine its value with relative confidence within the feasible parameter space based on the model output produced. However, the values of sensitive parameters that produce a behavioural model output can be distributed over a range of the feasible parameter space and can change when estimated from different response modes (Wagener et al., 2001). Hence MCAT uses an identifiability analysis, which is based either on simple inspection of the ‘dotty plots’ of Monte-Carlo outputs for a given parameter, for example taken from the upper performance quantile, or from an automated analysis.

The performance using different objective functions can be visualised using the ‘Multi Objective plot’ function in MCAT. The best performing parameter sets will not necessarily be the same for different objective functions. In this situation a ‘trade-off’ can be identified between the best performing parameter sets with respect to each objective function. Points which lie along this trade-off form the Pareto set, where: ‘a solution is said to be Pareto optimal (i.e. part of the Pareto set) if the value of any objective function cannot be improved without degrading at least one of the other objective functions’ (Chankong and Haimes, 1993). The MCAT can be used to determine the parameter values of the Pareto set and plot the model simulations produced by it against the observed time series. Finally, the GLUE (Beven and Binley, 1992) procedure, based on the RSA outlined above, can be used within the toolbox to define confidence limits in output time-series.

For both flow and water quality, calibration and prediction periods were assessed using the Nash–

Sutcliffe criteria (Nash and Sutcliffe, 1970):

$$R^2 = 1 - \frac{\sum_{i=1}^N (o_i - p_i)^2}{\sum_{i=1}^N (o_i - \bar{o})^2} \quad (12)$$

where  $o_i$  is the  $i$ th observed output variable,  $p_i$  is the  $i$ th predicted output variable,  $N$  is the number of observations and the overbar denotes the mean for the period of evaluation. Note that the Nash–Sutcliffe criteria has a basic reliance on the square of the errors, which thus focuses on fitting peak values.

The flow model was calibrated to find an optimum set of parameters  $K$ ,  $\alpha$ ,  $c$ ,  $d$  for an optimum number of cells,  $n$ . In addition, given the possible uncertainties in estimation of ungauged inflows, an ‘Inflow’ term was added to the flow model calibration procedure and is represented by a fixed percentage of the upstream flow rate for the calibration period.

Two principle methods of calibrating the water quality component of the model were used to illustrate both the relative suitability of the two methods and the strengths and weaknesses of the model structure. The first method involved the *sequential* calibration of the rate coefficients in Eqs. (3)–(5) (note the absence of ammonium as this determinand was not available in the data set used in this work). It should be noted that both the rate coefficients  $K_1^0$  (Eq. (3)) and  $K_5^0$  (Eq. (4)) are present also in Eq. (5), therefore the optimum calibrated values of  $K_1^0$  (Eq. (3)) and  $K_5^0$  (Eq. (4)) are placed directly into Eq. (5) and the rest of the rate coefficients in Eq. (5) then calibrated.

Note that the value of the photosynthetic oxygen production,  $P$ , (Eq. (5)) varies with time and is dependent on temperature, chlorophyll-a and solar radiation. However as no solar radiation data are available,  $P$  has been optimised directly assuming a constant value (recognising that this is a relatively crude assumption). Note that temperature (Eq. (1)) has no water quality rate coefficients to calibrate and is uniquely determined by the flow parameter  $T_p$ .

The second calibration approach is a *simultaneous* calibration procedure in which  $K_1^0$  (Eq. (3)) and  $K_5^0$  (Eq. (4)) are calibrated together with the other rate coefficients in Eq. (5). It should be noted that in the *sequential* method,  $K_1^0$  and  $K_5^0$  are determined independently of the other rate coefficients; in the *simultaneous* method they can be dependent. It may be expected that sequential and simultaneous

calibration should yield similar optimum parameters, but the procedure adopted allows for the investigation of parameter interactions.

## 5. Bedford Ouse case study

### 5.1. Study reach description

An application of the proposed model utilising the MCAT was undertaken using data from the river Ouse in eastern England (commonly known as the Bedford Ouse) between Tickford Abbey and Harrold Mill (flow) and Tickford Abbey and Sherington (water quality). The component catchment areas are 66.6 km<sup>2</sup> (Broughton Brook), 800.0 km<sup>2</sup> (River Ouse—Newport Pagnell), 277.1 km<sup>2</sup> (River Ouzel) and 1320.0 km<sup>2</sup> (River Ouse—Harrold Mill). The largest catchment—Harrold Mill—experiences a mean annual rainfall of some 656 mm. The reach length between River Ouse (Newport Pagnell) and Harrold Mill (Fig. 1) is some 27.1 km and the reach length between Tickford Abbey and Sherington is some 2.6 km. Previous work on this river is reported by Whitehead et al. (1979) who provide a more detailed description of the area.

The flow gauging stations at River Ouse (Newport Pagnell) and Harrold Mill (Fig. 1) define the upstream and downstream boundaries of the system, respectively. Fig. 2 shows the observed upstream and downstream hydrographs utilised in the modelling procedure. The overall upstream hydrograph is considered to be equal to the sum of the individual upstream hydrographs for the River Ouse (Newport Pagnell), River Ouzel and Broughton Brook, whilst the downstream hydrograph is the observed hydrograph at Harrold Mill. However, the hydrograph at Broughton Brook for this period was not recorded and consequently the hydrograph at this point was established by factoring the flow data for the River Ouzel in proportion to the area of the catchments. As the Broughton Brook catchment is quite small (66.6 km<sup>2</sup>) when compared with the River Ouzel catchment (277.1 km<sup>2</sup>) this is considered adequate for the present purpose. Tickford Abbey and Sherington represent the upstream and downstream boundaries for the water quality component of the modelling procedure as no water quality data were available at

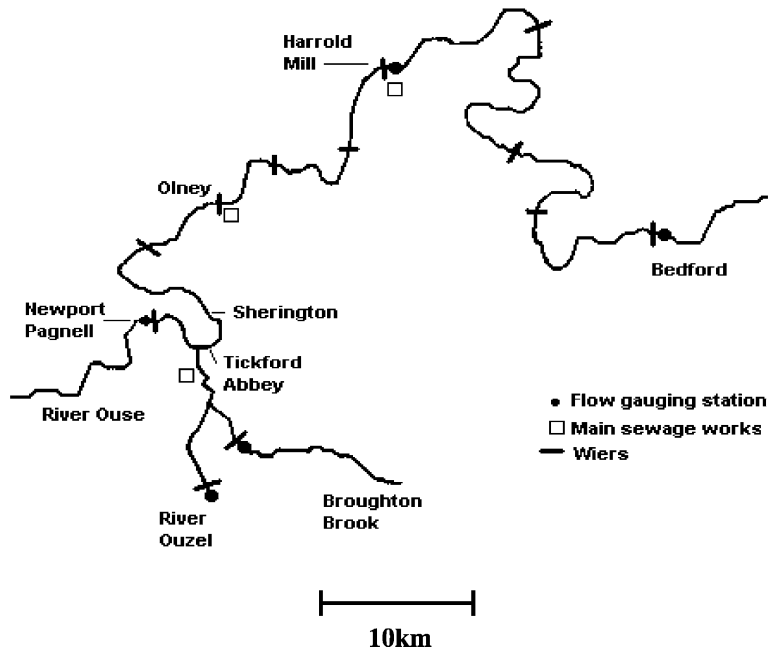


Fig. 1. The study area.

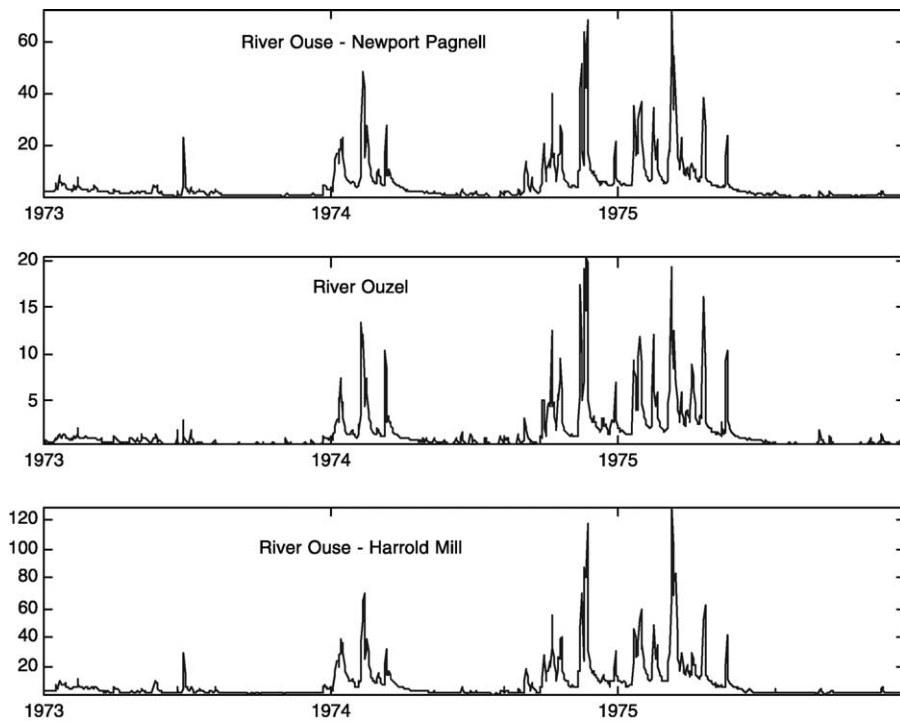


Fig. 2. Observed discharges on the Bedford Ouse for 1973, 1974 and 1975.

either of the flow gauging stations. Both flow and water quality data were generally available for years 1973, 1974 and 1975 at daily intervals, although there were time periods for which some or all of the water quality determinands were not recorded.

## 5.2. Modelling methodology

The flow component of the model was calibrated between upstream and downstream gauging stations using data from 27th August to 21st December 1974. The flow component of the model was then validated between 19th February and 15th June 1975. Note that unsteady flow periods were chosen for the flow calibration, although the periods available were limited due to gaps in the recorded data. The water quality component of the model was calibrated between Tickford Abbey and Sherington for the same period as the flow component using the correctly proportioned residence time predictions obtained from the calibrated flow parameters to obtain the calibrated rate coefficients (Eqs. (3)–(5)). Note that as the residence time is only around 2–3 h for the 2.6 km stretch used for assessing water quality behaviour and that flow data are only available at 24 h intervals, the model breaks down the daily water quality behaviour into hourly components via direct linear interpolation of the calibrated daily time series.

Ammonium was not included, due to the fact that most of the observed upstream and downstream concentrations were recorded as being  $<0.2 \text{ mg l}^{-1}$  and therefore realistic calibration and validation of ammonium behaviour was impractical. Where ammonium levels were required in the calibration of other water quality determinands for the periods in which these ammonium levels were recorded in error, the ammonium level was set to a default value of  $0.2 \text{ mg l}^{-1}$ . The optimum calibrated flow and water quality parameters were used in predictive mode for the period 1st April–15th June 1975.

## 6. Calibration and prediction results

### 6.1. Flow model component calibration

Uniform random parameter sampling for 20,000 simulations was undertaken to identify the region

representing an  $R^2$  value greater than 0.9 (i.e.  $1 - R^2$  below 0.1), used here to define the behavioural set. Initial attempts indicated that the lag term,  $\tau_{fl}$  (where  $\tau_{fl} = cQ^d$ ), had no effect on the behaviour of the flow model. The lag term was therefore dropped, resulting in a four parameter model ( $K$ ,  $\alpha$ ,  $n$  and an Inflow term), and the travel time of the non-conservative pollutant,  $T_p$ , is given by

$$T_p = m(nk_{nl}) \quad (13)$$

The value of  $n$  was determined by direct calibration (i.e. trials of number of cells ranged from 1 upwards until no performance advantage was gained by increasing the number of cells further in this case) and the best results were obtained for a single cell. Fig. 3 shows the behavioural Monte-Carlo results for the three optimised flow model parameters for  $n$  equal to 1 (the minima are marked by a small square). Feasible values of the parameter  $K$  range over the majority of the calibration values. The Inflow term has a well-defined minimum. The minimum value of the exponent  $\alpha$  is only very slightly non-linear (1.032 as opposed to 1 for a linear store), and equivalent performance is obtained over a range from 0.8 to 1.2, hence had a linear store been used the calibration procedure would not have produced radically different parameters for this particular river. We also observe a reduction in the number of parameter sets that yield accurate calibration results as the value of  $\alpha$  increases above 1. A calibration fit of  $R^2 = 0.9841$  is encouraging. Fig. 4 displays a RSA (Hornberger and Spear, 1981; Spear and Hornberger, 1980) of the behavioural flow model parameters. Ten quantile groups are ranked from the highest to the lowest likelihood, with the dark solid line indicating the best calibration fit. The storage coefficient  $K$  and the  $\alpha$  term are more sensitive within the model structure than the Inflow term, as shown by the larger difference between the cumulative frequency distributions. Fig. 5 shows the calibration and validation fit for the flow model (see also Table 1). Both calibration ( $R^2 = 0.9841$ ) and validation ( $R^2 = 0.9366$ ) performance is generally excellent, with the exception of the peaks which are systematically underestimated.

### 6.2. Water quality model component

Twenty thousand simulations were undertaken for each water quality determinand, with ranges for



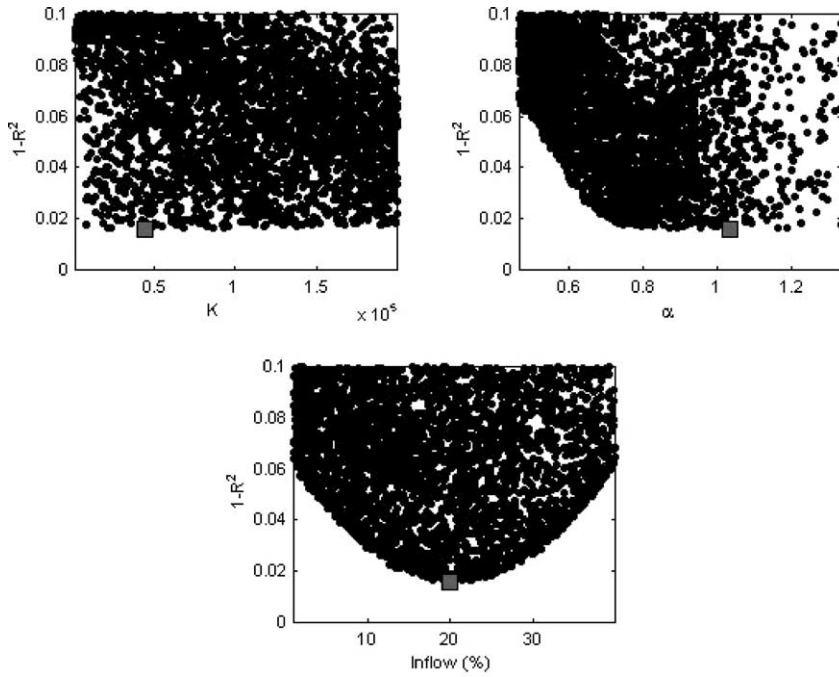


Fig. 3. Flow model parameters calibrated with respect to  $1 - R^2$ .

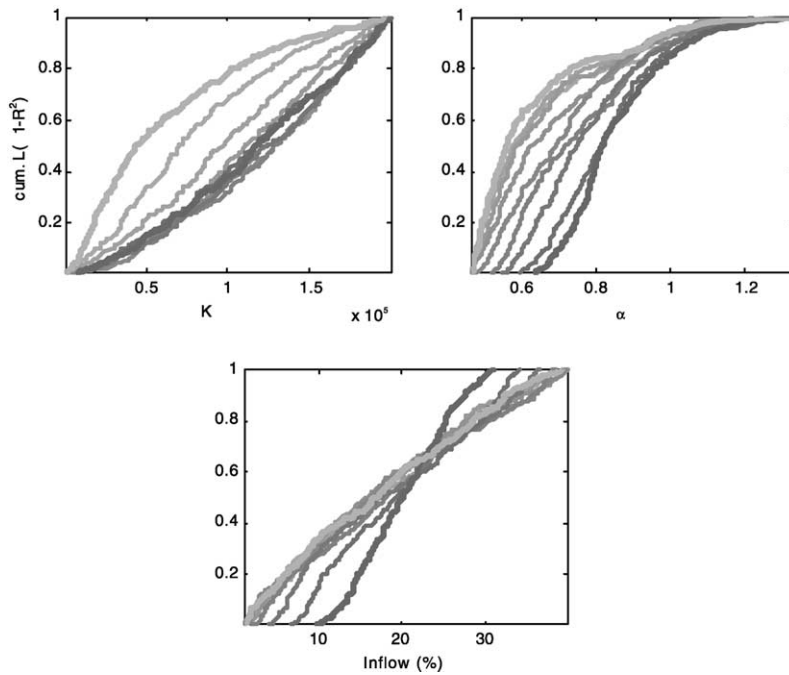


Fig. 4. Regional sensitivity plot of the calibrated flow model parameters.

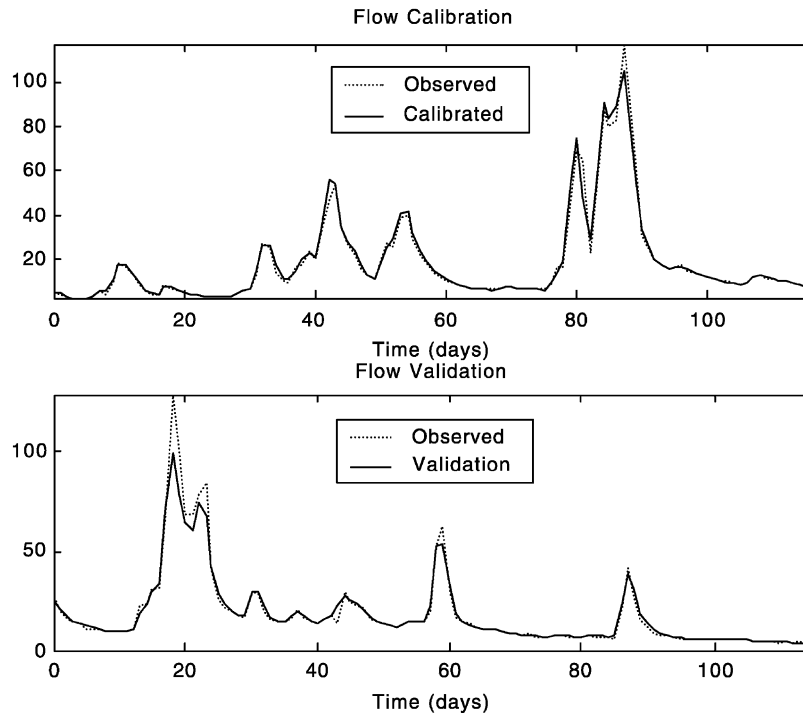


Fig. 5. Flow model calibration and validation for the period 27th August–21st December 1974 and 19th February–15th of June 1975, respectively.

the rate coefficients being those obtained by Williams (1994) and Lewis et al. (1997) in their work using the QUASAR model with UK catchments under comparable conditions. Note that a threshold of  $1-R^2 = 1.0$  is selected, with any result outside this limit being considered non-behavioural.

6.2.1. Nitrate

As can be noted from Fig. 6,  $K_2^0$ , the denitrification rate coefficient, appears to be better defined than  $K_1^0$ , the nitrification rate coefficient. Note that the implication of  $K_1^0$  being zero is that no nitrification is identifiable in the calibration period chosen for the Bedford Ouse. Elaborating on the reasons why the various water quality model parameters could not be identified from the calibration data, it is proposed that the reason behind the nitrification coefficient being zero is a result of the very low ammonium concentrations at the model boundaries. The simulation results (see also Table 1) indicate that the calibration procedure has produced a fit of good

quality ( $R^2 = 0.914$ ) with most local and the overall maxima being reasonably well re-produced.

6.2.2. BOD

Fig. 7 indicates that for sequential calibration both  $K_5^0$  (the rate coefficient for the loss of BOD) and  $K_{10}$  (the sedimentation rate coefficient) are well defined with the optimum values being near zero and at zero,

Table 1  
Calibration results for the period of the 27th of August 1974 to the 21st of December 1974 and flow validation results for the 19th of February to the 15th of June 1975

Calibration	$R^2$
Flow	0.9841
Temperature	0.9866
Nitrate	0.9141
BOD	0.4813
DO—sequential	0.9463
DO—non-sequential	0.9486
Validation	
Flow	0.9366

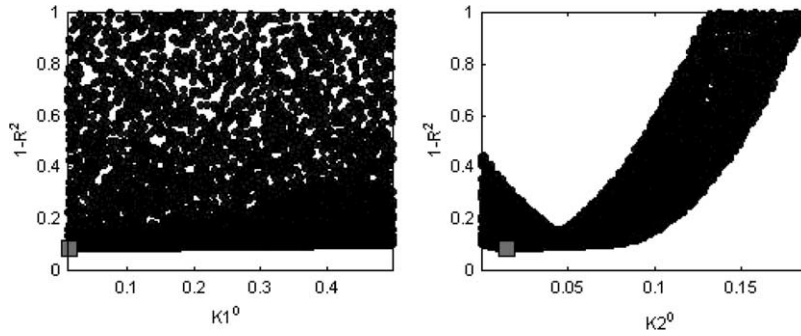


Fig. 6. Sequentially calibrated nitrate water quality model parameters.

respectively. This indicates that there is little apparent loss of BOD by decay and none by sedimentation during the calibration period.  $K_{11}$ , the rate coefficient for the BOD contribution by algae, does not have a well defined minimum. Fig. 8 shows use of the GLUE methodology to generate 95% confidence limits for the output. The bottom graph is added to make the identification of regions with large uncertainties easier, and represents the normalised width of the confidence limits (Lees and Wagener, 2000). Fig. 8 indicates that whilst some of the observations are within the GLUE uncertainty envelope, the majority are outside, indicating that the model is not calibrating

with confidence. The model has overestimated the observed maximum, but this may be due to the fact that the data were only recorded on a daily timescale; a short duration event may not have been detected.

6.2.3. DO—sequential calibration

Fig. 9 indicates that  $P$  is well defined; the same cannot be said for the other parameters of the DO model. Sequential calibration results (Table 1) give a fit of  $R^2 = 0.946$  demonstrating good calibration performance. It is interesting to note that as both  $K_8$  and  $K_9$  are completely insensitive

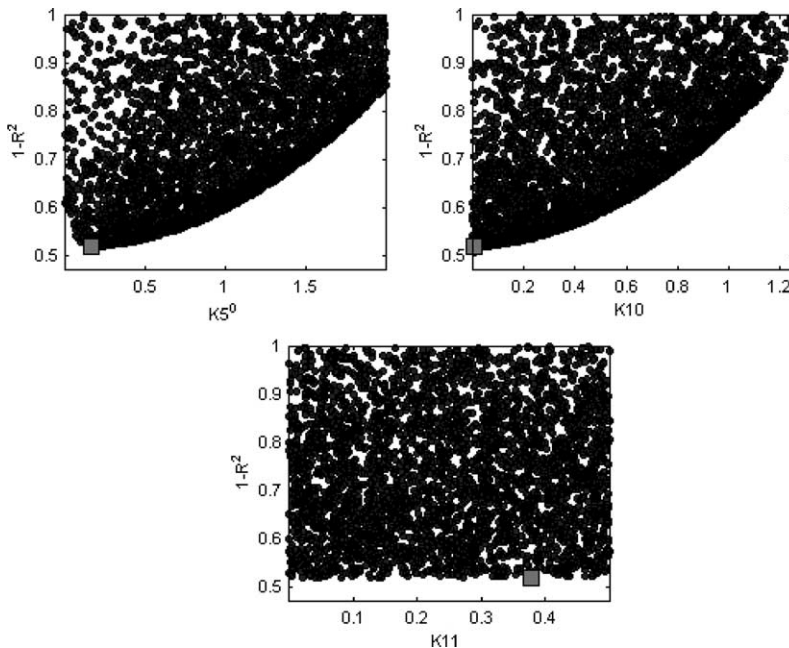


Fig. 7. Sequentially calibrated BOD water quality model parameters.

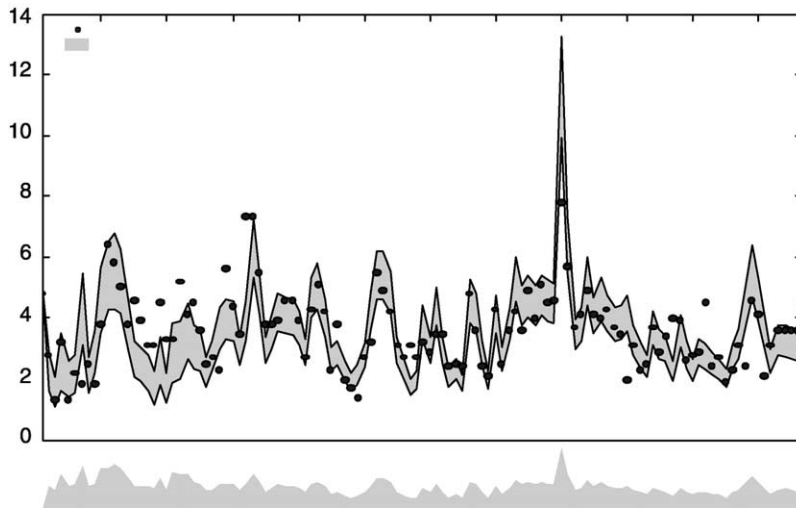


Fig. 8. GLUE output uncertainty limits for the sequentially calibrated BOD water quality model.

they make no meaningful contribution to the model performance.

6.2.4. DO—simultaneous calibration

Here all of the parameters of the DO model are optimised in a single calibration exercise.

Note from Fig. 10 that while  $P$ ,  $K_1^0$  and  $K_5^0$  are well defined,  $K_8$ ,  $K_9$  (algae respiration descriptors) and  $K_3^0$  (sediment oxygen uptake coefficient) are not. Non-sequential calibration results (Table 1) give a calibration fit of  $R^2 = 0.948$ , demonstrating only very slightly better calibration

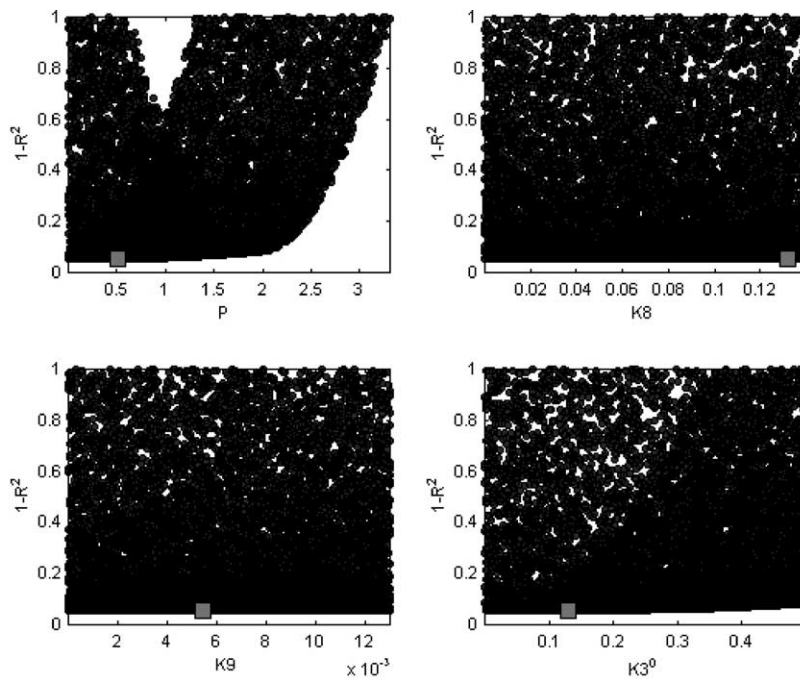


Fig. 9. Sequentially calibrated DO water quality model parameters.

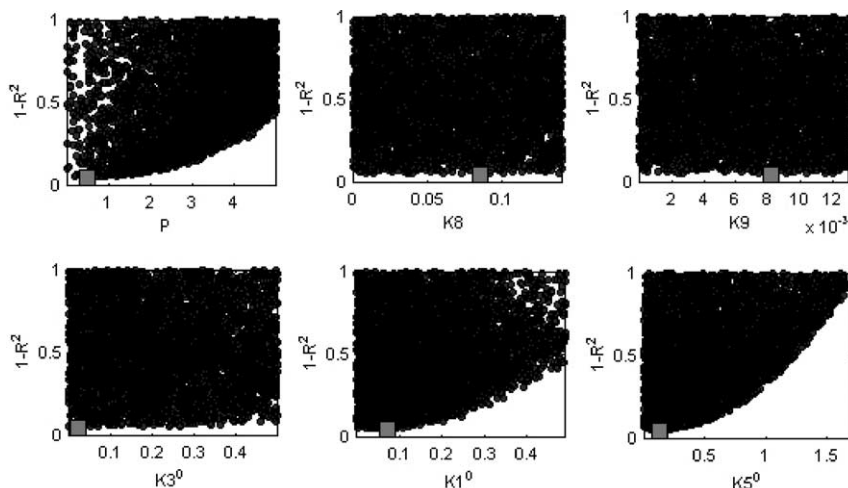


Fig. 10. Non-sequentially calibrated DO water quality model.

performance than for the sequential calibration ( $R^2 = 0.946$ ).

### 6.3. Water quality prediction under unsteady flow conditions

Fig. 11 shows that temperature has been predicted accurately ( $R^2 = 0.9361$ ) and nitrate behaviour less so ( $R^2 = 0.6466$ ). The most encouraging aspect is that the overall maxima and most local maxima have been predicted reasonably accurately. Similar traits are seen for the BOD prediction with an  $R^2 = 0.5068$ . Both the sequential and non-sequential predictions for DO are nearly identical ( $R^2 = 0.2355$  and  $0.3203$ , respectively). All prediction results are summarised in Table 2.

### 6.4. Multi-objective analysis

The sequential and non-sequential DO calibration and predictions have in fact produced near identical results, which is encouraging in that it points to a robust model framework. The degree of trade off between the calibration of the optimum value of  $K_1^0$  for the nitrate model and  $K_1^0$  for the DO model and  $K_5^0$  for the BOD model and  $K_5^0$  for the DO model may be investigated by the use of a 'Pareto front' as mentioned earlier in the text

(Chankong and Haimes, 1993). This is done by calibrating (using a Monte-Carlo procedure) both the nitrate, BOD and DO models independently (using the same objective function,  $1 - R^2$  in this case) and then plotting the results against each other in order to view the Pareto front. The results are shown below in Fig. 12, with the larger dots representing the results on the Pareto front. This indicates that there is some trade off between the optimum value of  $K_1^0$  for the nitrate and DO models, but the optimum values for  $K_5^0$  for the BOD and DO model are identical. The trade off between the optimum value of  $K_1^0$  for the nitrate and DO models is a source of concern as this indicates that the model structure is incapable of producing both the optimum behaviour of nitrate and DO within the same framework. However, there is no trade off between the optimum value of  $K_5^0$  for the BOD and DO models which indicates that both BOD and DO behaviour can be accurately assessed within the water quality model framework.

## 7. Conclusions

The calibration and validation of the flow component of the model has indicated that the performance of such a model is capable of simulating

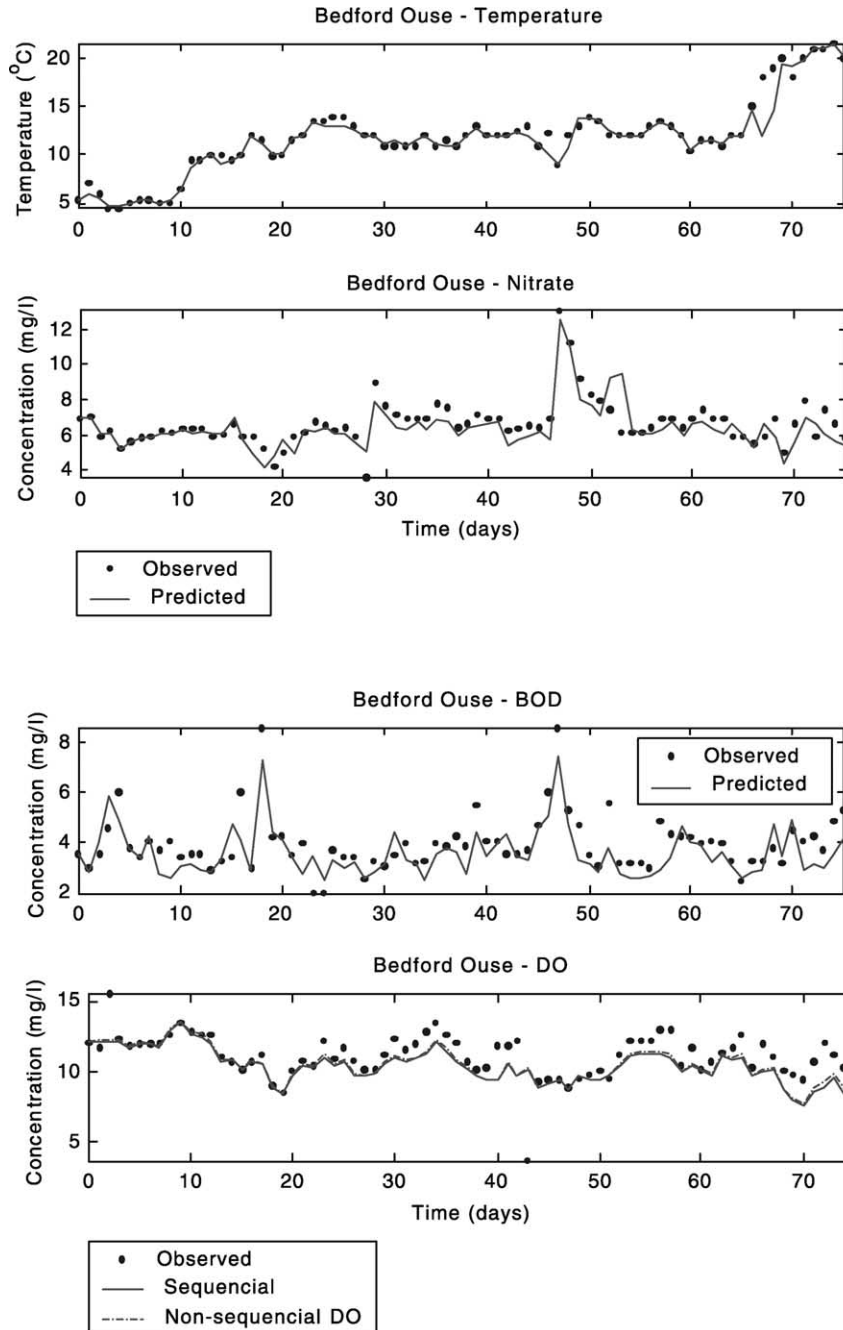


Fig. 11. Predicted temperature, nitrate BOD and DO at Sherington for the period of the 1st of April to the 15th of June 1975.

unsteady flow events with a reasonable degree of accuracy. Both sequential and non-sequential calibration and validation approaches used in the DO water quality component yield similar results—

although the non-sequential approach gave a slightly more accurate prediction. RSA has proved to be an extremely useful method for identifying which water quality and flow parameters may be considered to be

Table 2  
Prediction results at Sherington for the 1st of April to the 15th of June 1975

Prediction	$R^2$
Temperature	0.9361
Nitrate	0.6466
BOD	0.5068
DO—sequential	0.2355
DO—non-sequential	0.3203

the most important for the model performance. For example insensitive parameters within a given water quality model may be fixed at a single value and used in the predictive process with confidence, as opposed to selecting an arbitrary value from a wide range of possibilities. Despite the lack of information describing the photosynthetic oxygen production,  $P$ , a reasonably accurate water quality calibration and prediction process has been possible.

The most important implications of this work are that (1) several water quality model parameters are clearly unidentifiable—namely  $K_8$ ,  $K_9$  (algae respiration descriptors) and  $K_{11}$  (BOD contribution by

algae) and (2) other water quality model parameters such as  $K_1^0$  (nitrification rate coefficient) and  $K_{10}$  (sedimentation rate coefficient) were found to be equal to zero—i.e. the processes were not apparent during the calibration period. Further calibration exercises need to be undertaken in order to highlight how common such redundancy is, but the process implications are obviously significant.

The use of multiple objective functions (the Pareto front) provides a meaningful insight into the trade off regions which exist in the water quality model. Whilst the trade off between the optimum value of  $K_1^0$  for the nitrate and DO models is a source of concern, there is no trade off between the optimum value of  $K_5^0$  for the BOD and DO models, which indicates that both BOD and DO behaviour can be accurately assessed within the water quality model framework. Furthermore the essential framework of the QUASAR water quality model has been seen to be capable of accurately reproducing the water quality determinands under consideration in this case. Methods developed in this paper are generic and not limited solely to QUASAR. The lack of fine temporal water quality data is a source

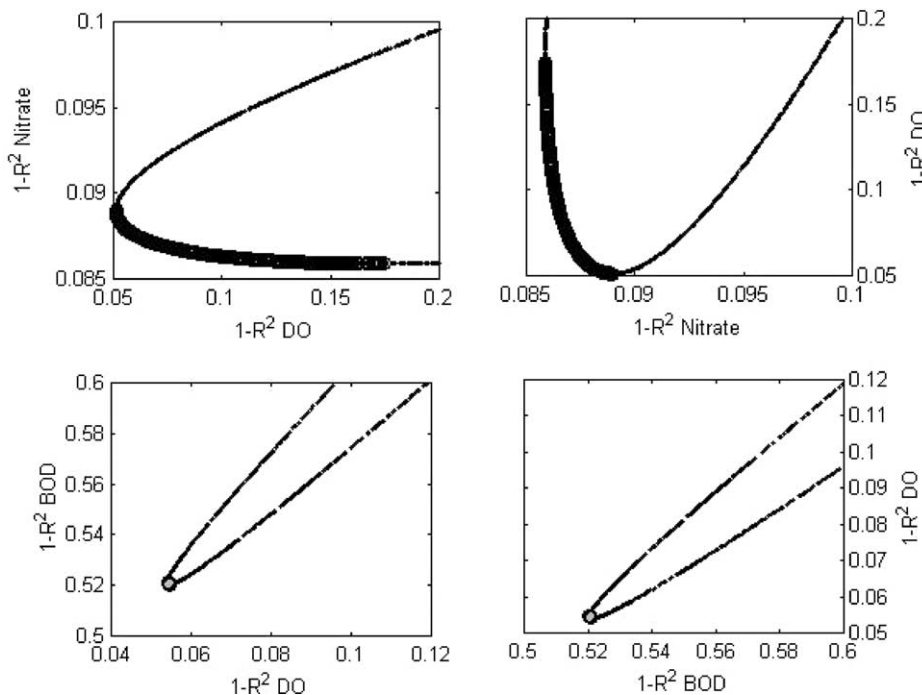


Fig. 12. 'Pareto front' (i.e. the 'trade-off' region) for nitrate and DO models (top) and for BOD and DO models (bottom).

of concern as it is hard to pin down the processes without a detailed time scale. The analytical methods used here in application to water quality problems have proved to be extremely useful in identifying which water quality and flow parameters may be considered to be the most important for the model performance.

### Acknowledgements

The first author would like to thank the EPSRC for granting financial support to this project under studentship No. 98806405 and also the Centre for Ecology and Hydrology for making the flow data available which was much appreciated. Many thanks to Neil McIntyre, Matthew Lees and Thorsten Wagener of Imperial College for their help and valued comments. The MCAT is available for download from <http://ewre.cv.ic.uk>. The first author would be interested to locate similar data sets to the one used here.

### References

- Beven, K.J., 2000. *Rainfall-Runoff Modelling—The Primer*, Wiley, New York.
- Beven, K.J., Binley, A.M., 1992. The future of distributed models: model calibration and uncertainty prediction. *Hydrological Processes* 6, 279–298.
- Bentura, P.L.F., Michel, C., 1997. Flood routing in a wide channel with a quadratic lag and route method. *Hydrological Sciences—Journal-des Sciences Hydrologiques* 42, 169–185.
- Camacho, L.A., Lees, M.J., 1999. Multilinear discrete lag-cascade model for channel routing. *Journal of Hydrology* 226, 30–47.
- Chankong, V., Haimes, Y.Y., 1993. Multiple optimization: Pareto optimality. In: Young, P.C., (Ed.), *Concise Encyclopedia of Environmental Systems*, Pergamon Press, Oxford, UK, pp. 387–396.
- Chapra, S.C., 1997. *Surface water-quality modeling*. McGraw-Hill, New York, NY.
- Freer, J., Beven, K.J., Ambrose, B., 1996. Bayesian estimation of uncertainty in runoff prediction and the value of data: an application of the GLUE approach. *Water Resources Research* 32 (7), 2161–2173.
- Gupta, H.V., Sorooshian, S., Yapo, P.O., 1998. Toward improved calibration of hydrologic models: multiple and non-commensurable measures of information. *Water Resources Research* 34 (4), 751–763.
- Hornberger, G.M., Spear, R.C., 1981. An approach to the preliminary analysis of environmental systems. *Journal of Environmental Management* 12, 7–18.
- Lees, M.J., Wagener, T., 2000. *The Monte Carlo Analysis Toolbox—User manual*. Imperial College of Science Technology and Medicine, London, UK. Unpublished at present, to be made available shortly.
- Lewis, D.R., Williams, R.J., Whitehead, P.G., 1997. Quality simulation along rivers (QUASAR): an application to the Yorkshire Ouse. *The Science of the Total Environment* 194, 399–418.
- Mathworks, 1996. *Matlab reference Guide*. Natick, Mass.
- Nash, J.E., Sutcliffe, J.V., 1970. River flow forecasting through conceptual models. Part I—a discussion of principles. *Journal of Hydrology* 10, 282–290.
- Permul, M., 1994. Multilinear discrete cascade model for channel routing. *Journal of Hydrology* 158, 135–150.
- Sincock, A.M., Lees, M.J., 2002. Extension of the QUASAR river water quality model to unsteady flow conditions. *The Journal of the Chartered Institute of Water and Environmental Management (CIWEM)* 16 (1), 12–17.
- Spear, R.C., Hornberger, G.M., 1980. Eutrophication in Peel Inlet, II, Identification of critical uncertainties via generalized sensitivity analysis. *Water Research* 14, 43–49.
- Wagener, T., Boyle, D.P., Lees, M.J., Wheat, H.S., Gupta, H.V., Sorooshian, S., 2001. A framework for the development and application of hydrological models. *Hydrology and Earth System Sciences* 5 (1).
- Wheat, H.S., Beck, M.B., 1995. Modelling upland stream water quality: process identification and prediction uncertainty. In: Trudgill, S., (Ed.), *Solute Modelling in Catchment Systems*, Wiley, New York, pp. 305–324.
- Wheat, H.S., Jakeman, A.J., Beven, K.J., 1993. Progress and directions in rainfall-runoff modelling. In: Jakeman, A.J., Beck, M.B., McAleer, M.J. (Eds.), *Modelling Change in Environmental Systems*, Wiley, New York, pp. 101–132.
- Whitehead, P.G., Young, P.C., Hornberger, 1979. A systems model of stream flow and water quality in the Bedford Ouse River—1. Stream flow modelling. *Water Research* 13, 1155–1169.
- Whitehead, P.G., Williams, R.J., Lewis, D.R., 1997. Quality simulation along river systems (QUASAR): model theory and development. *The Science of the Total Environment* 194/195, 447–456.
- Williams, R.J., 1994. *QUASAR Technical Guide V2.0: Notes on Calibrating QUASAR*, Institute of Hydrology.